
Optical and Quantum Electronics **32:** 473–487, 2000.

Femtosecond pulse processing

A. M. WEINER
Purdue University, School of Electrical and Computer Engineering, West Lafayette, IN 47907-1285
(E-mail: amw@ecn.purdue.edu)

Abstract. We discuss Fourier methods for shaping and processing femtosecond optical signals. Examples of applications in optical communications and in generation of terahertz radiation are presented.

Key words: optical communications, pulse shaping, terahertz radiation, ultrafast optics

1. Introduction

A variety of powerful femtosecond pulse processing methods, based on a time-domain Fourier optics approach, have been developed over the last ten years (Weiner 1995; Weiner and Kanan 1998). This paper gives a brief overview of selected results from this field, drawing upon work by the author. In Sect. 2 we discuss Fourier transform pulse shaping, which allows synthesis of femtosecond optical waveforms according to specification. Then in Sect. 3 we review holographic and non-linear pulse processing experiments, which enable storage, recall, convolution and correlation of femtosecond optical waveforms, as well as space-time conversion operations. Systems utilizing space-time conversions in conjunction with smart pixel optoelectronic device arrays may lead to a new paradigm for switching and processing of high-speed time-division-multiplexed optical data. In Sect. 4 we discuss recent results on a direct space-to-time pulse shaper, which may be particularly suitable for space-time processing systems. Finally, in Sect. 5 we discuss applications of pulse shaping for generation of terahertz radiation.

2. Femtosecond pulse shaping

We first discuss femtosecond pulse shaping, in which powerful Fourier synthesis methods are utilized to generate almost arbitrarily shaped femtosecond optical waveforms (Weiner *et al.* 1988a; Weiner 1995). As sketched in Fig. 1, in pulse shaping an incident femtosecond pulse is spread into its constituent spectral components by a grating and lens. A spatially patterned mask then modulates the phase and amplitude of the spatially dispersed spectral components. After the spectral components are recombined by a second lens and grating, a shaped output pulse is obtained, with the pulse shape given by

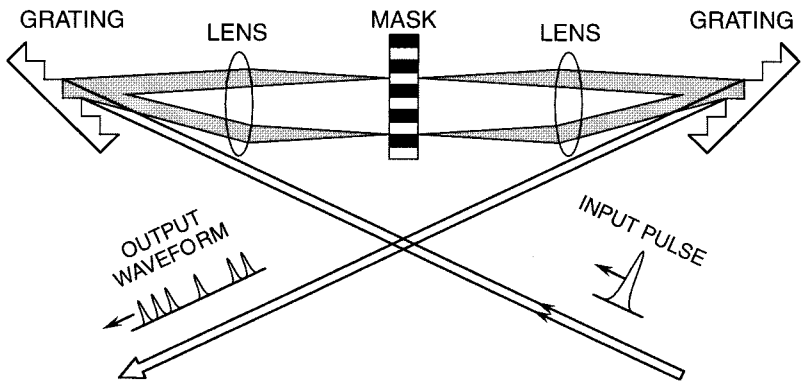

Fig. 1. Femtosecond pulse shaping apparatus.

the Fourier transform of the pattern transferred by the mask onto the spectrum. Pulse shaping masks have been implemented by using microlithographic patterning techniques (Weiner *et al.* 1988a, b), programmable spatial light modulators (Weiner *et al.* 1992a; Hillegas 1994; Wefers and Nelson 1995), holographic masks (Nuss and Morrison 1995), and deformable mirrors (Heritage *et al.* 1991; Zeek *et al.* 1999). Pulse shaping has been successfully applied for a variety of experiments in laboratories worldwide, with applications ranging from high-speed communications to ultrafast spectroscopy and high-field physics.

Pulse shaping has many potential applications for broadband communications. One simple example is the possibility of generating packets of ultrashort 'bits' for transmission in time-division multiplexed (TDM) transmission or networking systems. The intensity profile of a short pulse sequence consisting of four ones, a zero, and four ones, with a peak pulse repetition rate in the Tbit/s range, is shown in Fig. 2 (Weiner and Leaird 1990). This particular waveform was generated by using a fixed phase-only filter fabricated using microlithographic patterning techniques. One goal of our current research is to produce such waveforms using one-dimensional optoelectronic modulator arrays, so that new packets can be formed and reprogrammed on a subnanosecond time scale. A direct space-to-time pulse shaper particularly useful for this goal is discussed in Sect. 4.

A second application is dispersion compensation with application to ultrashort pulse fiber transmission. In our group we have recently demonstrated transmission of sub-500-femtosecond pulses over a 2.5 km link consisting of lengths of standard single-mode fiber (SMF) and dispersion compensating fiber (DCF) (Chang and Weiner 1997). By carefully matching both the dispersions and dispersion slopes, we obtain less than a factor of two pulse broadening, despite the fact that the pulse first broadens by several hundred-fold in the SMF part of the link. An example of our data is shown in

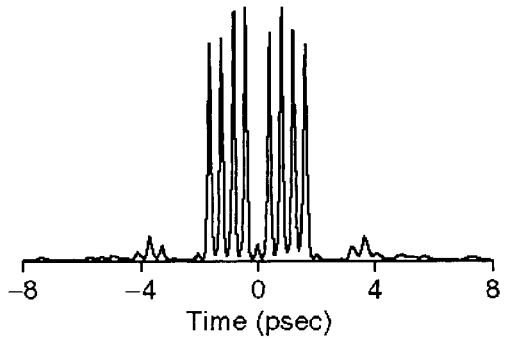

Fig. 2. Ultrafast optical pulse ('bit') sequence, generated through femtosecond pulse shaping.

Fig. 3. Due to a small residual dispersion slope in our link, the output pulse in Fig. 3(b) has an asymmetric distortion characteristic of dispersion slope. We can compensate for this phase distortion by programming a pulse shaper

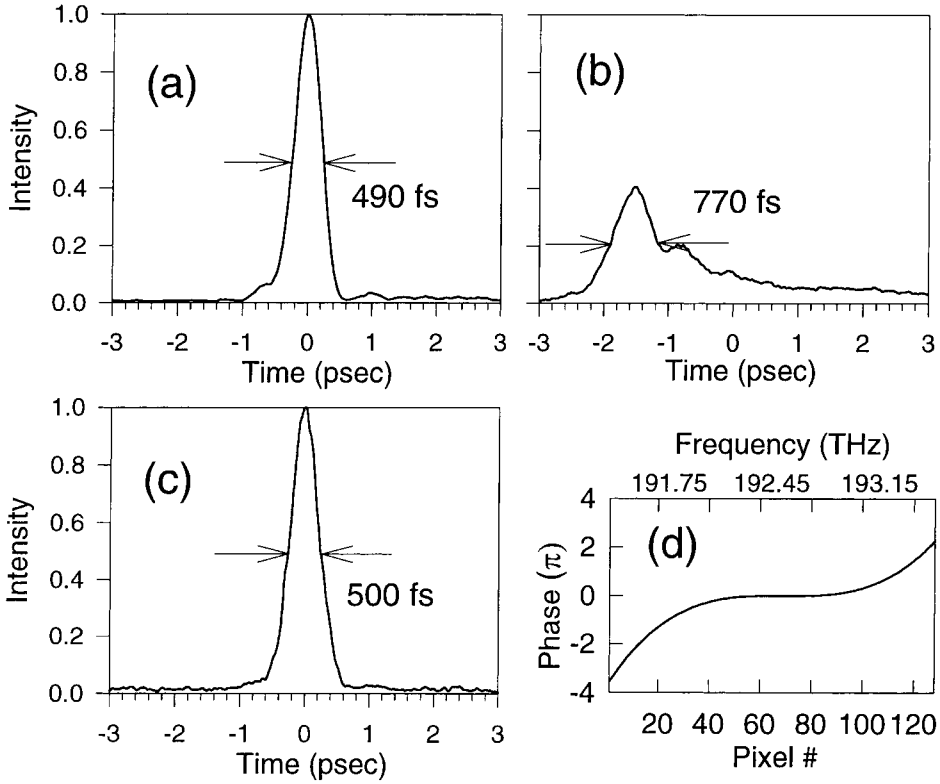

Fig. 3. Input pulse to the 2.5-km fiber link (a) and output pulse from the fiber link when constant phase (b) or cubic phase correction (c) is applied to LCM. The applied phase pattern is shown in (d).

for an equal and opposite cubic phase. This is implemented using a fiber pigtailed pulse shaper, with a low fiber-to-fiber insertion loss of 5.3 dB, with a 128-element liquid crystal phase modulator (Weiner *et al.* 1992a) as the programmable mask. The applied spectral phase function is shown in Fig. 3(d). The resulting pulse, shown in Fig. 3(c), is completely recompressed with no observable distortion (Chang *et al.* 1998). We have recently extended this technique to shorter pulses (400 fs) and longer fiber spans (10 km), again with no observable distortion (Shen and Weiner 1999). This technique for fine tuning out small amounts of residual dispersion from dispersion compensated links should be applicable both to code-division multiple-access (CDMA) (Chang *et al.* 1998; Sardesai *et al.* 1998) and ultrahigh-speed TDM optical transmission and networking. The use of a pulse shaper in a similar fashion to compensate spectral phase distortions in high power femtosecond amplifier systems has also been reported recently by several groups (Brixner *et al.* 1998; Efimov *et al.* 1998; Zeek *et al.* 1999).

The ability to program a pulse shaper under computer control has also led recently to several interesting demonstrations of adaptive pulse shaping (Bardeen *et al.* 1997; Baumert *et al.* 1997; Yelin *et al.* 1997; Assion *et al.* 1998; Brixner *et al.* 1998; Efimov *et al.* 1998; Meshulach *et al.* 1998). In these experiments one starts with a random spectral pattern programmed into the pulse shaper, which is updated iteratively according to a stochastic optimization algorithm based on the difference between a desired and measured experimental output. In this way, femtosecond waveform synthesis or chirp compensation can be achieved without the need to explicitly program the pulse shaper.

It is also worth noting that pulse shapers have also been used for applications in wavelength-division-multiplexed (WDM) communications. Here the pulse shaper is used to realize programmable and nearly arbitrary spectral filters, e.g., for equalization of the gain spectrum of erbium-doped fiber amplifiers (Ford and Walker 1998) and for implementation of a multiwavelength optical switch with nearly square passbands (Patel and Silberberg 1995). Interestingly, integrated optical components designed for WDM applications are also being adapted to implement integrated optical pulse shapers (Fermann *et al.* 1993; Kurokawa *et al.* 1997; Takenouchi *et al.* 1998).

3. Holographic and non-linear Fourier pulse processing

Pulse shaping can be extended to accomplish more sophisticated pulse processing operations by including holographic or non-linear materials in place of a mask or spatial light modulator within the pulse shaping apparatus. For example, by using a pair of input beams to the pulse shaper, one can write a

spectral hologram, which allows storage, recall, time-reversal and matched filtering of ultrafast temporal signals as well as correlations and convolutions between pairs of ultrafast signals (Mazurenko 1990; Weiner *et al.* 1992b). As one recent example, Fig. 4 shows data demonstrating holographic correction of pulse broadening due to a spectral phase distorter (Ding *et al.* 1998). Note that in these experiments, the holographic medium was a dynamic photorefractive quantum well material with response time as fast as microseconds, which allows the spectral holography setup to adaptively track slow variations in the input pulse. Undistorted input pulses (Fig. 4a) have a measured width of 260 fs, while the diffracted output pulses (Fig. 4c) have measured widths of 410 fs, where the pulse broadening results only from the limited optical bandwidth of the excitonic non-linearity in the photorefractive quantum wells. Figure 4c shows the measurement of a broadened and distorted pulse generated by passing it through a pulse shaper containing a phase aberrator. The diffracted output from the spectral holography setup (Fig. 4d), with 407 fs width is essentially unchanged from the non-distorted input pulse case. This illustrates the correlation and matched filtering operations of spectral holography, which can occur automatically in a self-aligned manner. Slow variations in pulse timing were also adaptively corrected in

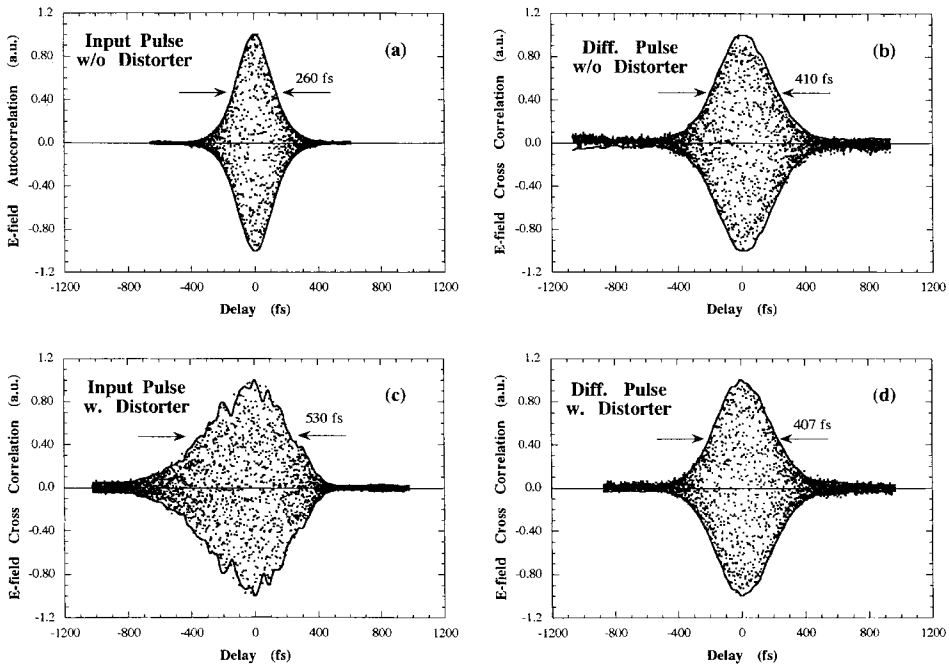

Fig. 4. Electric field cross-correlation data for the input signal-pulse without (a) and with the phase distorter (c), and the corresponding diffracted output pulse from the hologram (b and d).

these experiments (Ding *et al.* 1998). In addition to pure time-domain processing, spectral holography can also be applied to implement time-to-space (Ema *et al.* 1991; Nuss *et al.* 1994; Sun *et al.* 1997; Kanan and Weiner 1998) or space-to-time (Ema and Shimizu 1990; Sun *et al.* 1995; Ding *et al.* 1997; Marom *et al.* 1999) (serial-to-parallel or parallel-to-serial) conversion operations.

For applications where faster update rates are required, such as packet processing for ultrafast optical communications and networking, operation on a nanosecond time scale or faster is desired. Holographic materials are generally too slow for this. We are currently pursuing subnanosecond update rates in pulse shaping and processing in two ways:

- For space-to-time conversion, we have demonstrated a pulse shaping geometry in which the output temporal waveform is a direct replica of the spatial masking function (as opposed to the Fourier transform relation of the pulse shaper shown in Fig. 1) (Leaird and Weiner 1999). This geometry is compatible with the use of one-dimensional optoelectronic modulator arrays for high-speed operation, and tests using high-speed optoelectronics are now under way. Experiments demonstrating operation of this direct space-to-time pulse shaper on a femtosecond time-scale are briefly reviewed in Sect. 4.
- For time-to-space conversion, we have adopted an apparatus in which a second harmonic crystal within the pulse shaper replaces the holographic material used by earlier time-to-space experiments. Since second harmonic generation (SHG) is an instantaneous non-linearity, very high-speed operation is possible provided a sufficient power budget is available. This geometry was first demonstrated by Mazurenko, Fainman, and coworkers (Sun *et al.* 1997). We have recently performed similar time-to-space conversion experiments (Kanan and Weiner 1998; Weiner and Kanan 1998), where we have demonstrated a second harmonic conversion efficiency of 58%, a more than 500-fold enhancement compared to the earlier experiments. Key to obtaining this high efficiency was the realization that inside a pulse shaper, where the spectral components are dispersed, the pulse width is correspondingly increased, and therefore, group velocity mismatch (GVM) in the second harmonic crystal is not a significant issue. This allows the use of a much thicker non-linear crystal than in the usual femtosecond experiments, where GVM is a serious effect. The use of a thicker crystal with a high non-linearity in a non-critical phase matching geometry is responsible for the greatly increased SHG efficiency. High conversion efficiency will be very important for construction of time-space processing systems operating with reasonable power levels at frame rates suitable for high-speed communications.

One current objective is to further exploit the relationship between time and space in pulse shaping and spectral holography in conjunction with space-domain smart pixel optoelectronic processing. Our concept is shown in Fig. 5

(Weiner and Kanan 1998). High-speed time-domain signals will be converted into the space-domain, processed using smart pixel arrays, and then converted back to the ultrafast time-domain. We envision that by integrating the processing power of parallel electronics and optoelectronics into our system in this way, a number of sophisticated new operations (e.g., time slot interchange, digital logic) will become possible for ultrafast and broadband optical signals.

4. Direct space-to-time pulse shaper

The direct space-to-time (DST) pulse shaper (Leaird and Weiner 1999) has two important advantages for high-speed pulse sequence generation, compared to the Fourier transform pulse shaper, as follows:

1. It avoids the need to perform a Fourier transform to determine the masking function for each new packet, which would be very difficult at high update rates. Instead, there would be a one-to-one mapping between an individual modulator element and an individual bit in the output data packet, which would be ideal for parallel-to-serial conversion of data in byte or word format.
2. Data packet generation using Fourier transform shaping typically requires that both spectral amplitude and phase be precisely controlled. Pulse sequence generation with a DST shaper requires only intensity modulation, which is compatible with existing optoelectronic modulator array technologies.

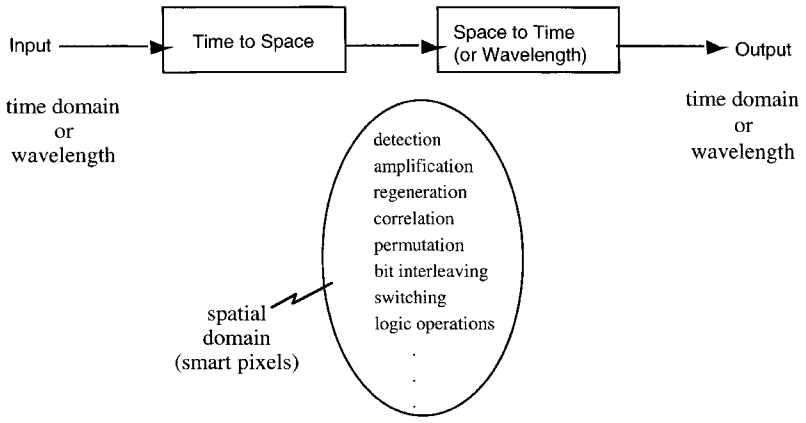

Fig. 5. Block diagram of generalized space-time pulse processing systems. By converting interchangeably between time, space and wavelength domains, sophisticated data manipulation applications may be possible.

We note that the concept of a DST pulse shaper was previously demonstrated for simple waveforms on a picosecond time scale by Emplit *et al.* (1987, 1992). Here we demonstrate generation of optical data packets on a femtosecond time scale (Leaird and Weiner 1999), in a geometry compatible with direct insertion of a high-speed optoelectronic modulator array.

Figure 6 shows a schematic representation of the direct space-to-time shaper. Although this system has some similarities to the conventional Fourier transform pulse shaper, there are also distinct differences. In particular, the Fourier plane of the lens contains a thin slit, and the spatially patterned mask is placed at the diffraction grating. The field of the input pulse just prior to being dispersed by the diffraction grating (at plane P1 in Fig. 6) is simply the field of the laser input transmitted through the spatially patterned mask:

$$e_1(x,t) \propto \int \mathrm{d}\omega\, E_{\mathrm{in}}(\omega) s(x) \mathrm{e}^{j\omega t} \tag{1}$$

Here $s(x)$ is the spatial profile at P1, given by the input beam spatial profile multiplied by the transmission through the spatially patterned mask and $E_{\mathrm{in}}(\omega)$ is the Fourier transform of the input field $e_{\mathrm{in}}(t)$. The diffraction grating disperses this spatially patterned input field, and the lens performs a spatial Fourier transform on the dispersed frequency components. At the Fourier plane of the lens (P2), the spatial profile of any particular frequency component is the Fourier transform of the input spatial profile:

$$e_2(x,t) \propto \int \mathrm{d}\omega\, E_{\mathrm{in}}(\omega) S(\beta(x - \alpha\omega)) \mathrm{e}^{j\omega t} \tag{2}$$

Here $S(k)$ is the Fourier transform of the spatial profile at the grating, $\alpha = \lambda^2 f / 2\pi c d \cos\theta_{\mathrm{d}}$ is the spatial dispersion, and $\beta = (2\pi/\lambda f)(\cos\theta_{\mathrm{d}}/\cos\theta_{\mathrm{i}})$ is the Fourier transform scaling factor including the beam size change upon diffraction from the grating, f denotes the focal length of the pulse shaping lens, d is the period of the diffraction grating, c is the speed of light, λ is the center wavelength and θ_{d} and θ_{i} are the diffraction and incident angles, respectively. The thin slit samples the spectrally dispersed frequency com-

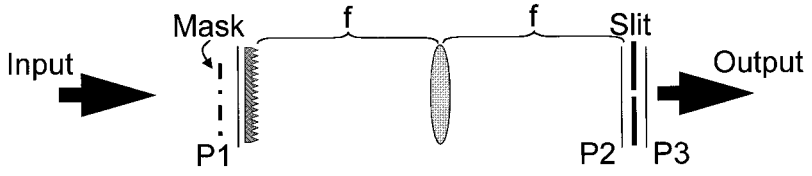

Fig. 6. Schematic representation of pulse shaping components in the direct space-to-time shaper.

ponents (around $x = 0$) giving a spatially uniform output spectrum that is the Fourier transform of the input spatial profile. The result is:

$$e_3(t) \propto \int \mathrm{d}\omega\, E_{\mathrm{in}}(\omega) S(-\alpha\beta\omega) \mathrm{e}^{j\omega t} \propto e_{\mathrm{in}}(t) * s(-t/\alpha\beta) \tag{3}$$

The temporal profile is simply determined by the input pulse convolved with a scaled representation of the input spatial profile, with the space-to-time scaling constant (unit ps/mm) given by:

$$\alpha\beta = \frac{\lambda}{cd \cos\theta_{\mathrm{i}}} \tag{4}$$

Figure 7 shows an example of a pulse train generated using the DST pulse shaper. A fixed amplitude mask, fabricated using standard lithographic techniques to pattern a gold layer deposited onto a glass substrate, was used at the input of the shaper. The transmission mask consists of various linear arrays of 20 μm transparent rectangles with 62.5 μm center-to-center spacing. The space between the transparent rectangles is opaque due to the gold film. Figure 7 shows a cross-correlation measurement of the optical pulse sequence generated with pixelation mask pattern consisting of a periodic arrays of 20 μm transparent rectangles. Clearly there are twenty uniformly spaced temporal pulses. The separation between pulses (1.88 ps) is in excellent agreement with the expected conversion constant, which was calculated by modifying Equation (4) to include the magnification of the optical system imaging the actual mask onto the grating. The roll-off in the temporal profile toward the edges of the train is due to the finite size of the Gaussian beam at the pixelation mask. Similar experiments, demonstrating generation of ultrafast optical data packets with some of the twenty pulses in Fig. 7 turned off, have also been reported (Leaird and Weiner 1999).

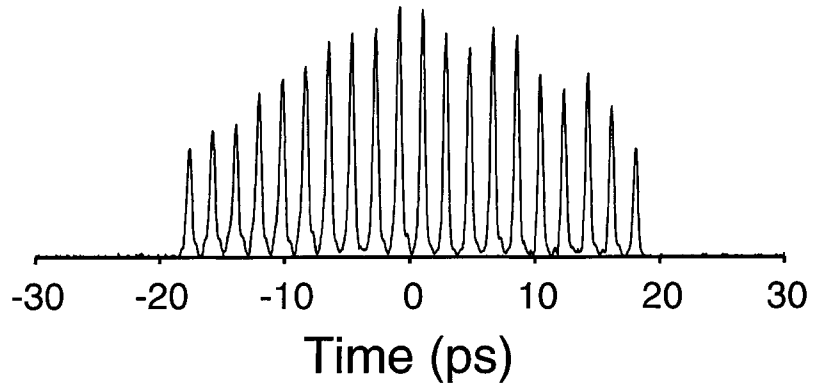

Fig. 7. A 20-pulse 'optical comb' generated with fixed mask.

5. Applications for generation of terahertz (THz) radiation

Shaped femtosecond pulses have important applications in ultrafast laser–matter interactions and spectroscopy. Within my group sequences of femtosecond pulses generated by pulse shaping were previously applied for selective amplification of coherent optical phonons through multiple-pulse impulsive stimulated Raman scattering (Weiner *et al.* 1990) and for multiple-pulse excitation and control of coherent quantum mechanical charges oscillations in quantum well systems (Brener *et al.* 1993). More recently, the use of shaped femtosecond pulses for manipulation and enhancement of optically excited THz radiation has been investigated. In one set of experiments, we demonstrated THz waveform synthesis by using shaped pulses to excite ultrafast photoconductive dipole antennas, resulting in generation of quasi-narrowband THz tone bursts and THz pulse trains with internal phase and amplitude modulations (Lin *et al.* 1996a). Two examples of THz waveform shaping are shown in Fig. 8. Figure 8(a) shows the intensity cross-correlation measurements of the shaped optical waveforms; in each case the optical signal is a six pulse sequence, but with different delays between the third and

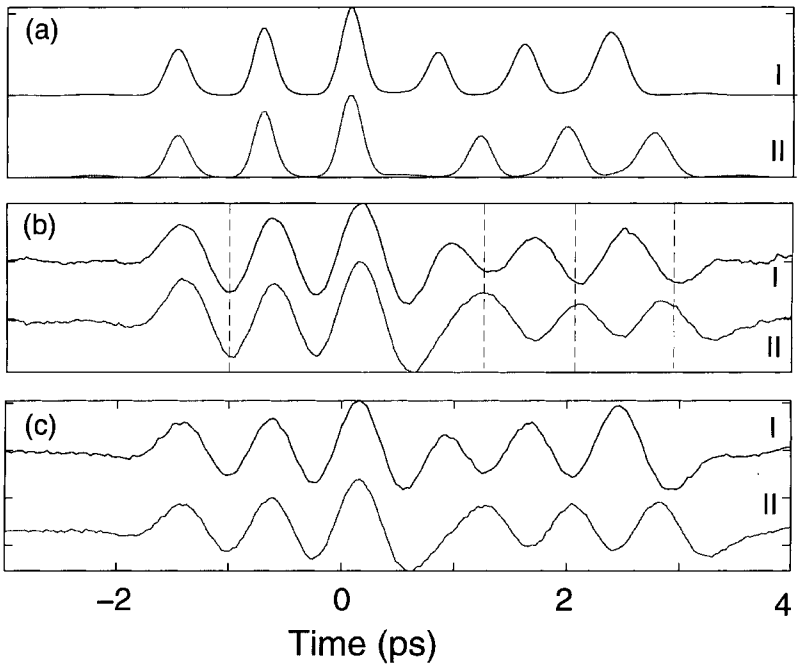

Fig. 8. (a) Measured intensity cross-correlations of two different optical pulse sequences, marked I and II. (b) Corresponding THz radiation waveforms measured via photoconductive sampling. The dashed lines highlight the phase shift within the THz waveforms controlled via an extra time delay between pulses three and four in optical pulse sequence II. (c) Calculated THz waveforms based on the cross-correlation data and the measured single-pulse THz system response.

fourth pulses. The resulting THz waveforms are shown in Fig. 8(b), where the change in optical pulse spacing leads to a phase modulation internal to the THz waveform. Theoretical THz waveforms, Fig. 8(c), calculated on the basis of the measured optical excitation waveforms, show good agreement with the experimental results.

We also discovered that multiple pulse excitation could result in an enhanced power spectral density at a selected THz frequency through avoidance of saturation effects (Liu *et al.* 1996b). Data illustrating this effect for the case of dipole antennas are shown in Fig. 9, which plots the Fourier transform of the detected THz waveforms for both single-pulse and multiple-pulse excitation at low (11 mW) and higher (44 mW) average optical excitation powers. Within each of the two plots, the average optical power for single and multiple-pulse excitation is kept the same. There are three main observations. First, multiple-pulse excitation converts the THz spectrum, which is broadband under single-pulse excitation, into a series of relatively narrow peaks corresponding to the pulse repetition frequency and its harmonics (only the lowest harmonic is visible in Fig. 9). Second, in the lower power case, the THz spectral peaks obtained under multiple-pulse excitation lie on the broadband THz envelope resulting from single-pulse excitation [Fig. 9(a)]. This effect is expected whenever the THz response is a linear function of the input optical intensity. Third, in the higher optical power case, saturation effects become evident; and we observe a significant enhancement in the peak THz spectrum under multiple-pulse excitation compared to the THz spectrum excited by a single-pulse [Fig. 9(b)]. There are two main saturation mechanisms which can limit THz emission from photoconductive antennas. One mechanism is screening of the applied bias field due to charge separation resulting from the photocurrent; this effect is reduced under multiple-pulse excitation due to rapid carrier trapping and recombination, which can take place in between pulses for fast photoconductors. The second mechanism is screening of the applied field by the THz field itself; this effect is reduced under multiple-pulse excitation due to the lower peak THz fields.

Recently, we have also extended this multiple-pulse excitation technique to enhance the THz emission from large aperture photoconductors driven by an amplified femtosecond source, which results in substantially higher peak electric fields (Siders *et al.* 1999). These experiments also elucidate the role of the photoconductor response time in avoidance of saturation due to screening by the THz field.

6. Summary

In summary, we have given a brief overview of the field of Fourier optics femtosecond pulse processing, drawing on examples of work from the

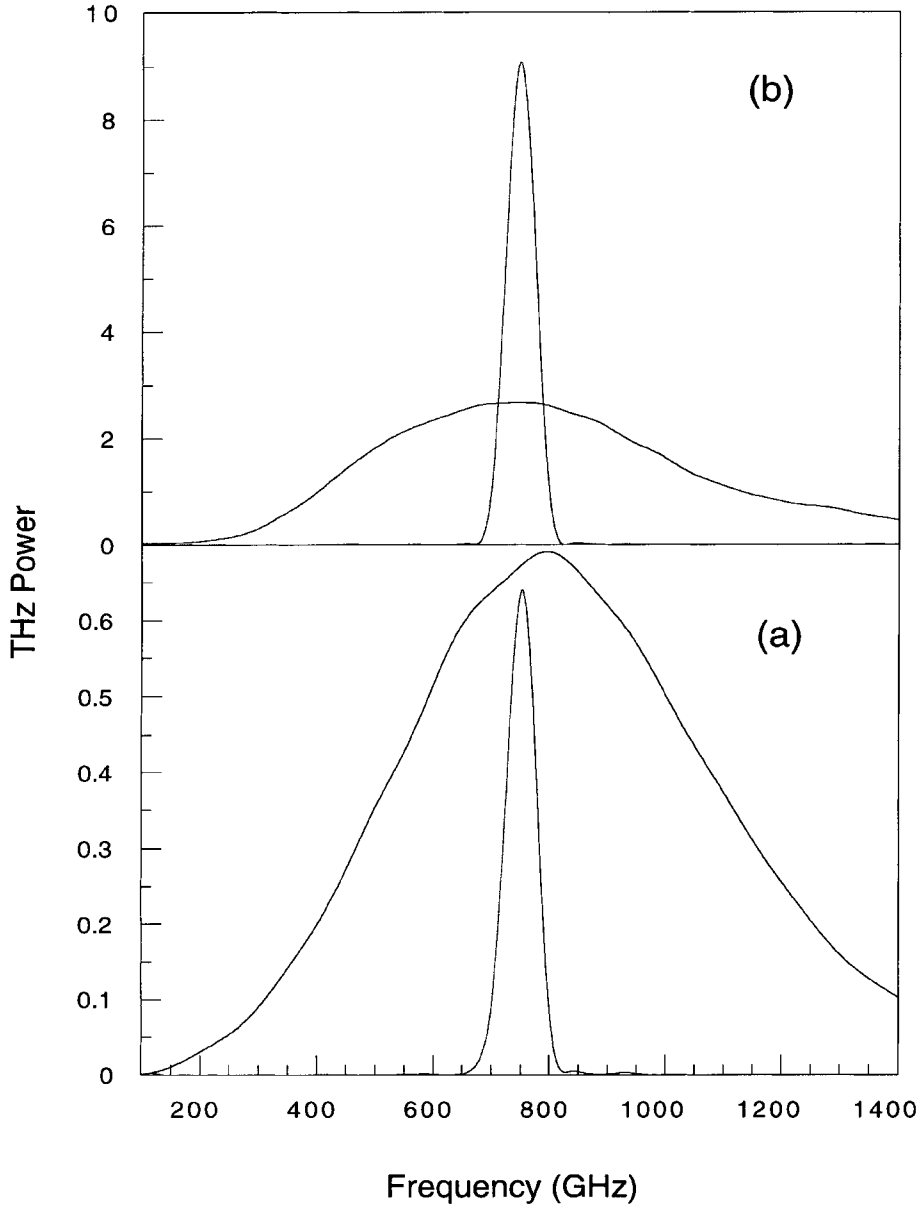

Fig. 9. Power spectra of THz radiation resulting from broadband single-pulse excitation and narrowband multiple-pulse excitation, for (a) 11 mW average optical power (bottom) and (b) 44 mW average optical power (top). For the higher optical input power case, a clear enhancement in the peak spectral power density is observed when using multiple-pulse excitation.

author's laboratory. We first described femtosecond pulse shaping, which allows nearly arbitrary spectral filtering and waveform synthesis of femtosecond optical signals, with applications such as dispersion compensation

and code-division multiple-access communications. We also discussed extensions of pulse shaping incorporating holographic or non-linear media within the pulse shaper, which lead to femtosecond pulse processing operations such as correlation, matched filtering, and space-to-time and time-to-space conversions. Finally, we illustrated the application of pulse shaping in spectroscopy and ultrafast laser–matter interactions by describing its use for manipulation and enhancement of THz radiation from photoconductive antennas.

Acknowledgements

This work could not have been accomplished without the efforts of many talented collaborators. For the work highlighted in this paper, I would particularly like to acknowledge Jon Heritage for collaborating on the early pulse shaping work at Bellcore and Cheng-chun Chang, Yi Ding, Ayman Kanan, Dan Leaird, Yongquin Liu, Prof. Mike Melloch, Prof. Dave Nolte, Sang-Gyu Park, Harshad Sardesai, and Shuai Shen for their work on pulse shaping and processing and THz radiation at Purdue. I would also like to acknowledge support for this work from the Air Force Office of Scientific Research under F49621-05-1-0533, the Army Research Office under DAAG55-98-1-0514, and the National Science Foundation under 9626967-ECS and 9722668-PHY.

References

Assion, A., T. Baumert, M. Bergt, T. Brixner, B. Kiefer, V. Seyfried, M. Strehle and G. Gerber. Control of Chemical Reactions by Feedback-Optimized Phase-Shaped Femtosecond Laser Pulses. *Science* **282** 919–922, 1998.

Bardeen, C.J., V.V. Yakovlev, K.R. Wilson, S.D. Carpenter, P.M. Weber, and W.S. Warren. Feedback Quantum Control of Molecular Electronic Population Transfer. *Chem. Phys. Lett.* **280** 151–158, 1997.

Baumert, T., T. Brixner, V. Seyfried, M. Strehle and G. Gerber. Femtosecond Pulse Shaping by an Evolutionary Algorithm with Feedback. *Appl. Phys. B* **65** 779–782, 1997.

Brener, I., P.C.M. Planken, M.C. Nuss, L. Pfeiffer, D.E. Leaird and A.M. Weiner. Repetitive Excitation of Charge Oscillations in Semiconductor Heterostructures. *Appl. Phys. Lett.* **63** 2213, 1993.

Brixner, T., M. Strehle and G. Gerber. Feedback-Controlled Optimization of Amplified Femtosecond Laser Pulses. *Appl. Phys. B* **68** 281–284, 1998.

Chang, C.-C. and A.M. Weiner. Fiber Transmission for Sub-500-fs Pulses Using a Dispersion Compensating Fiber. *IEEE J. Quantum Electron.* **33** 1455–1464, 1997.

Chang, C.-C., H.P. Sardesai and A.M. Weiner. Code-Division Multiple-Access Encoding and Decoding of Femtosecond Optical Pulses Over a 2.5-km Fiber Link. *IEEE Phot. Tech. Lett.* **10** 171–173, 1998.

Chang, C.-C., H.P. Sardesai and A.M. Weiner. Dispersion-Free Fiber Transmission for Femtosecond Pulses Using a Dispersion-Compensating Fiber and a Programmable Pulse Shaper. *Opt. Lett.* **23** 283–285, 1998.

Ding, Y., D.D. Nolte, M.R. Melloch and A.M. Weiner. Real-Time Edge Enhancement of Femtosecond Time-Domain Images. *Opt. Lett.* **17** 1101–1103, 1997.

Ding, Y., D.D. Nolte, M.R. Melloch and A.M. Weiner. Spectral Holography for Dynamic Dispersion Compensation, presented at the Ultrafast Phenomena XI, Garmisch-Partenkirchen, Germany, 1998.

Efimov, A. and D.H. Reitze. Programmable Dispersion Compensation and Pulse Shaping in a 26-fs Chirped-Pulse Amplifier. *Opt. Lett.* **23** 1612–1614, 1998.

Efimov, A., M.D. Moores, N.M. Beach, J.L. Krause and D.H. Reitze. Adaptive Control of Pulse Phase in a Chirped-Pulse Amplifier. *Opt. Lett.* **23** 1915–1917, 1998.

Ema, K. and F. Shimizu. Optical Pulse Shaping Using a Fourier-transformed Hologram. *Jpn. J. Appl. Phys.* **29** 1458, 1990.

Ema, K., M. Kuwata-Gonokami and F. Shimizu. All-Optical Sub-Tbits/s Serial-to-Parallel Conversion Using Excitonic Giant Nonlinearity. *Appl. Phys. Lett.* **59** 2799–2801, 1991.

Emplit, P., J.-P. Hamaide and F. Reynaud. Passive Amplitude and Phase Picosecond Pulse Shaping. *Opt. Lett.* **17** 1358–1360, 1992.

Emplit, P., J.P. Hamaide, F. Reynaud, C. Froehly and A. Barthelemy. Picosecond Steps and Dark Pulses Through Nonlinear Single Mode Fibers. *Opt. Commun.* **62** 374–379, 1987.

Fermann, M.E., V.D. Silva, D.A. Smith, Y. Silberberg and A.M. Weiner. Shaping of Ultrashort Optical Pulses by Using an integrated Acousto-optic Tunable Filter. *Opt. Lett.* **18** 1501–1507, 1993.

Ford, J.E. and J.A. Walker. Dynamic Spectral Power Equalization Using Micro-Opto-Mechanics. *IEEE Phot. Tech. Lett.* **10** 1440–1442, 1998.

Heritage, J.P., E.W. Chase, R.N. Thurston and M. Stern. A Simple Femtosecond Optical Third-Order Disperser, presented at the Conference on Lasers and Electro-optics, Baltimore, MD, 1991.

Hillegas, C.W., J.X. Tull, D. Goswami, D. Strickland and W.S. Warren. Femtosecond Laser Pulse Shaping by Use of Microsecond Radio-Frequency Pulses. *Opt. Lett.* **19** 737–739, 1994.

Kanan, A.M. and A.M. Weiner. Efficient Time-to-Space Conversion of Femtosecond Optical Pulses. *J. Opt. Soc. Am. B* **15** 1242–1245, 1998.

Kurokawa, T., H. Tsuda, K. Okamoto, K. Naganuma, H. Takenouchi, Y. Inoue and M. Ishii. Time-Space Conversion Optical Signal Processing Using Arrayed Waveguide Grating. *Electron. Lett.* **33** 1890–1891, 1997.

Leaird, D.E. and A.M. Weiner. Femtosecond Optical Packet Generation via a Direct Space-to-Time Pulse Shaper. *Opt. Lett.* **24** 853–855, 1999.

Liu, Y., S.-G. Park and A.M. Weiner. Terahertz Waveform Synthesis via Optical Pulse Shaping. *IEEE J. Select Top. Quantum Electron.* **2** 709–719, 1996a.

Liu, Y., S.-G. Park and A.M. Weiner. Enhancement of Narrowband Terahertz Radiation from Photoconducting Antennas by Optical Pulse Shaping. *Opt. Lett.* **21** 1762–1764, 1996b.

Marom, D.M., D. Panasenko, P.C. Sun and Y. Fainman. Spatial-Temporal Wave Mixing for Space-Time Conversion. *Opt. Lett.* **24** 563–565, 1999.

Mazurenko, Y.T. Holography of wave packets. *Appl. Phys. B* **50** 101–114, 1990.

Meshulach, D., D. Yelin and Y. Silberberg. Adaptive Real-Time Femtosecond Pulse Shaping. *J. Opt. Soc. Am. B* **15** 1615–1619, 1998.

Nuss, M.C. and R.L. Morrison. Time-Domain Images. *Opt. Lett.* **20** 740–742, 1995.

Nuss, M.C., M. Li, T.H. Chiu, A.M. Weiner and A. Partovi. Time-to-Space Mapping of Femtosecond Pulses. *Opt. Lett.* **19** 664–666, 1994.

Patel, J.S. and Y. Silberberg. Liquid Crystal and Grating Based Multiple-Wavelength Cross-Connect Switch. *IEEE Phot. Tech. Lett.* **7** 514–516, 1995.

Sardesai, H.P., C.-C. Chang and A.M. Weiner. A Femtosecond Code-Division Multiple-Access Communication System Testbed. *J. Lightwave Technol.* **16** 1953–1964, 1998.

Shen, S. and A.M. Weiner. Complete Dispersion Compensation for 400-fs Pulse Transmission Over 10-km Fiber Link Using Dispersion Compensating Fiber and Spectral Phase Equalizer. *IEEE Phot. Tech. Lett.* **11** 827–829, 1999.

Siders, C.W., J.L.W. Siders, A.J. Taylor, S.-G. Park, M.R. Melloch and A.M. Weiner. Generation and Characterization of Terahertz Pulse Trains from Biased, Large Aperture Photoconductors. *Opt. Lett.* **24** 241–243, 1999.

Sun, P.C., Y.T. Mazurenko and Y. Fainman. Femtosecond Pulse Imaging: Ultrafast Optical Oscilloscope. *J. Opt. Soc. Am. A* **14** 1159, 1997.

Sun, P.C., Y.T. Mazurenko, W.S.C. Chang, P.K.L. Yu and Y. Fainman. All-Optical Parallel-to-Serial Conversion by Holographic Spatial-to-Temporal Frequency Encoding. *Opt. Lett.* **20** 1728–1730, 1995.

Takenouchi, H., H. Tsuda, K. Naganuma, T. Kurokawa, Y. Inoue and K. Okamoto. Differential Processing of Ultrashort Optical Pulses Using Arrayed Waveguide Grating with Phase-Only Filter. *Electron. Lett.* **34** 1245–1246, 1998.

Wefers, M.M. and K.A. Nelson. Generation of High-Fidelity Programmable Ultrafast Optical Waveforms. *Opt. Lett.* **20** 1047–1049, 1995.

Weiner, A.M. Femtosecond Optical Pulse Shaping and Processing. *Prog. Quantum Electron.* **19** 161–238, 1995.

Weiner, A.M. and A.M. Kanan. Femtosecond Pulse Shaping for Synthesis, Processing and Time-to-Space Conversion of Ultrafast Optical Waveforms. *IEEE J. Select. Top. Quantum Electron.* **4** 317–331, 1998.

Weiner, A.M. and D.E. Leaird. Generation of terahertz-Rate Trains of Femtosecond Pulses by Phase-only Filtering. *Opt. Lett.* **15** 51–53, 1990.

Weiner, A.M., J.P. Heritage and E.M. Kirschner. High-Resolution Femtosecond Pulse Shaping. *J. Opt. Soc. Amer. B* **5** 1563–1572, 1988a.

Weiner, A.M., J.P. Heritage and J.A. Salehi. Encoding and Decoding of Femtosecond Pulses. *Opt. Lett.* **13** 300–302, 1988b.

Weiner, A.M., D.E. Leaird, J.S. Patel and J.R. Wullert. Programmable Shaping of Femtosecond Pulses by Use of a 128-Element Liquid–Crystal Phase Modulator. *IEEE J. Quantum Electron.* **28** 908–920, 1992a.

Weiner, A.M., D.E. Leaird, D.H. Reitze and E.G. Paek. Femtosecond Spectral Holography. *IEEE J. Quantum Electron.* **28** 2251–2261, 1992b.

Weiner, A.M., D.E. Leaird, G.P. Wiederrecht and K.A. Nelson. Femtosecond Pulse Sequences Used for Optical Control of Molecular motion. *Science* **247** 1317, 1990.

Yelin, D., D. Meshulach and Y. Silberberg. Adaptive Femtosecond Pulse Compression. *Opt. Lett.* **22** 1793–1795, 1997.

Zeek, E., K. Maginnis, S. Backus, U. Russek, M. Murnane, G. Mourou and H. Kapteyn. Pulse Compression by Use of Deformable Mirrors. *Opt. Lett.* **24** 493–495, 1999.